

# PROPOSAL ON THE ELECTROSTATIC GUIDE BASED EXPERIMENTAL CHANNEL AT THE IBR-2 REACTOR

D.V. Kamanin<sup>1</sup>, Yu.V. Pyatkov<sup>1,2</sup>, A.A. Alexandrov<sup>1</sup>, V.S. Aleksandrov<sup>1</sup>, N. Jacobs<sup>3</sup>,  
N.Yu. Kazarinov<sup>1</sup>, E.A. Kuznetsova<sup>1</sup>, V.N. Shvetsov<sup>1</sup>, Ts. Panteleev<sup>1</sup>, Yu.V. Ryabov<sup>4</sup>

<sup>1</sup>Joint Institute for Nuclear Research, Dubna, Russia

<sup>2</sup>National Nuclear Research University "MEPHI", Moscow, Russia

<sup>3</sup>University of Stellenbosch, Faculty of Military Science, Military Academy, Saldanha 7395, South Africa

<sup>4</sup>Institute for Nuclear Research RAN, Moscow, Russia

## INTRODUCTION

In our previous works [1÷3] different modes of a new type of ternary decay of low excited heavy nuclei called collinear cluster tri-partition (CCT) were reported. In the most populated "Ni"-mode based on the magic isotopes of Ni (fig. 1) two CCT partners fly after scission almost collinearly with angular divergence of  $\sim 0.2^\circ$  (fig. 2). This mode was identified in the frame of the missing mass approach, i.e. only two out of three of more collinear partners were registered. However the direct detection of all three partners is very desirable for working out the physical model of the CCT process.

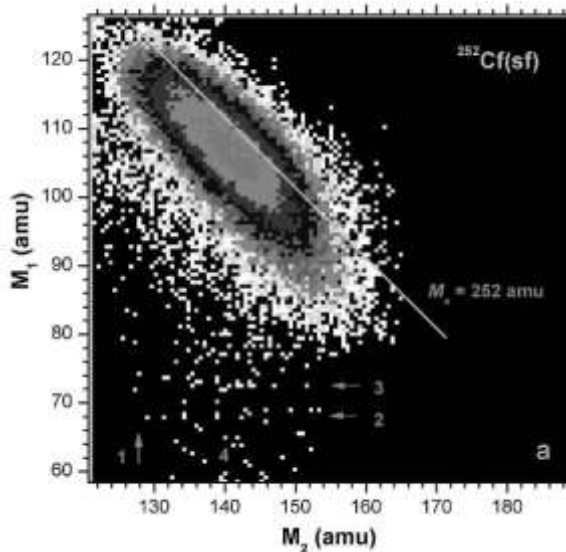


**FIGURE 1.** The region of the mass-mass distribution for the FFs from  $^{252}\text{Cf}$  (sf) around the CCT Ni-bump. It contains almost no background of scattered fragments. No selection conditions were applied. An internal structure of the "bump" is seen as the horizontal and tilted lines (marked by numbers 1÷4).

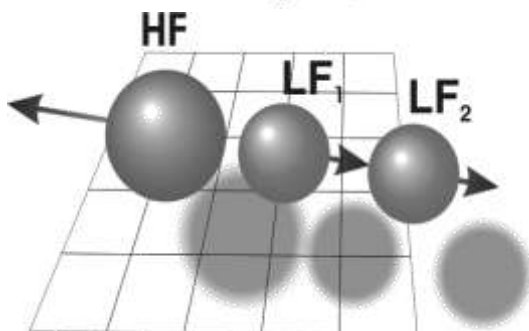


**FIGURE 2.** Kinematics of the CCT partners of one of the CCT modes. All three fragments marked as HF (the heaviest one), LF<sub>1</sub> and LF<sub>2</sub> (two lighter fragments) fly apart almost collinearly. marked as HF (the heaviest one), LF<sub>1</sub> and LF<sub>2</sub> (two lighter fragments) fly apart almost collinearly.

The detection of almost collinear fragments with the PIN diode mosaic is a very complicated experimental task because one has to mask the edges of the PIN diodes. The width of the mask between neighboring diodes put a limit for distinguishing two fragments which is for the moment amounts to approximately  $1^0$  and hardly can be decreased.

## ELECTROSTATIC GUIDE SYSTEM

We are going to use electrostatic guide system for transporting the fission fragments from the target in the vicinity of the IBR-2 active zone to the detectors placed in several meters from the target (fig. 3). Similar guide system has been already used at the reactor [4]. It was proposed for the first time in ref. [5]. The important difference of our proposal to the guides from [4, 5] is the double-armed design of the system (fig. 3). The registration of all the CCT partners in coincidence will allow the application of both the mass and momentum conservation laws for the identification of the ternary decays. Also the background will be drastically reduced.

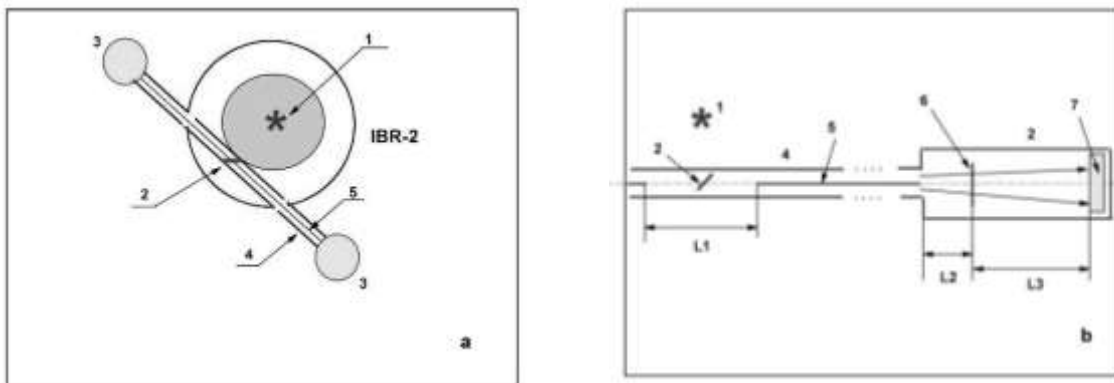


**FIGURE 3.** The layout of the setup (a) and the basic diagram of one arm with the experimental chambers at the end of the guide (b). 1 – active zone, 2 – target, 3 – detectors chambers, 4 – reactor channel, 5 – central filament of the guide, 6 – “start” detector, 7 – mosaic of PIN-diodes.

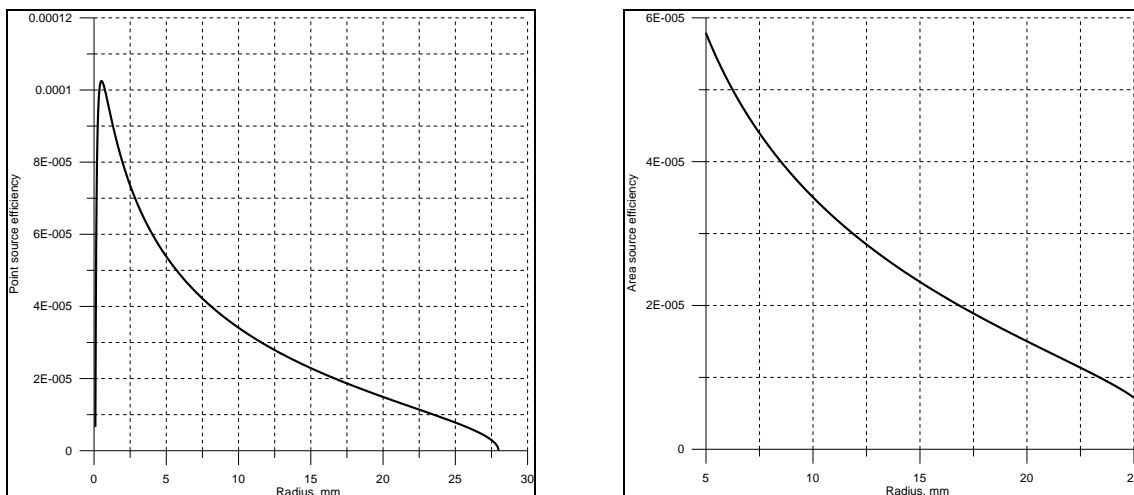


**FIGURE 4.** The guide transport efficiency for the point target (a) and for the target 5 mm in diameter (b) placed symmetrically at the guide start as a function of the radius from the central wire at the guide end.

According to [5] the collection efficiency  $F_c$  of the guide for an extended, uniform, target of radius  $b$  equal to the tube (outer cylinder) radius  $R$  is estimated to be:

$$F_c = 0.153q V_0 / \{E_{FF} \ln(R/s)\}, \quad (1)$$

where  $V_0$  is the potential difference between the two conductors,

$E_{FF}$  – is the kinetic energy of the fission fragment,

$s$  – is the radius of the central wire of the guide,

$q$  – ionic charge.

For instance in ref. [4] when the central electrode was under the potential of -2.5 kV the guide efficiency was 50 times higher than the geometrical one and amounted to  $1.5 \times 10^{-6}$ . The thermal neutron flux at the target position was about  $3.7 \times 10^{11} \text{ cm}^{-2} \text{ s}^{-1}$  what resulted in the detection of few fission fragments (FFs) per second using spectrometric targets.

For typical FF of the light mass peak the radial efficiency distribution of the guide (parameters are presented below) is illustrated by fig. 4.

## MODELING OF THE GUIDE SYSTEM

Evidently, for each ion with fixed parameters  $E_{FF}$  and  $q$  emitted at a given distance  $r_0$  from the center of the target there is some maximal angle  $\beta_{max}$  between its velocity and guide wire. It determines the size of the “acceptance cone”. Parameters  $E_{FF}, q, r_0, \beta < \beta_{max}$  at fixed value of  $V_0$  determine specific shape of the trajectory of the ion in the guide system. It is reasonable to suppose that two initially collinear CCT fragments differ by their energy  $E_{FF}$  and ionic charge  $q$  will distant from each other while moving along the guide.

In order to estimate the distance between the points where fragments hit the plane of the “stop” mosaic (fig. 3b) the special modeling was performed. The parameters of the fragments chosen for the modeling are presented in Table 1. In this selected two fragments ( $^{72}\text{Ni}$  and  $^{128}\text{Sn}$ ) have been really detected in the opposite arms of the spectrometer (see the left side of the rectangular structure in fig. 1a marked by number 1). The parameters of the third CCT partner ( $^{52}\text{Ca}$ ) were calculated basing on both mass and momentum conservation laws. The hypothetic values were chosen for the ionic charges being unknown from the experiment.

Table 1. Parameters of the collinear CCT fragments chosen for the modeling

Isotope	$M$ (amu)	$E$ (MeV)	$v$ (cm/ns)	$P$ (amu*cm/ns)	$q$ (units)	$E/q$ kV
$^{72}\text{Ni}$	72	21	0.75	54	16	1312.5
$^{52}\text{Ca}$	52	57	1.46	76	4	14250
$^{128}\text{Sn}$	128	68	1.01	130	22	3090.9

The other parameters used for the calculations are as follows:  $V_0 = 10 \text{ kV}$ ,  $s = 0.1 \text{ mm}$ , channel diameter (outer cylinder) is 56 mm, the length of one guide arm is 5 m, the target diameter is 5 mm.

As can be inferred from the table Ni fragment is the most “soft” for the guide system ( $\beta_{max} = 3.29^0$ ) among all three. The  $^{52}\text{Ca}$  ion which flies in the same direction has  $\beta_{max} = 0.998^0$ .

The 3D trajectories of the initially collinear ions of Ca and Ni emitted at the angle of  $\beta_{max}(\text{Ca})$  are presented in fig. 5. Fig. 6 shows the distance between the ions of Ca and Ni along the guide.

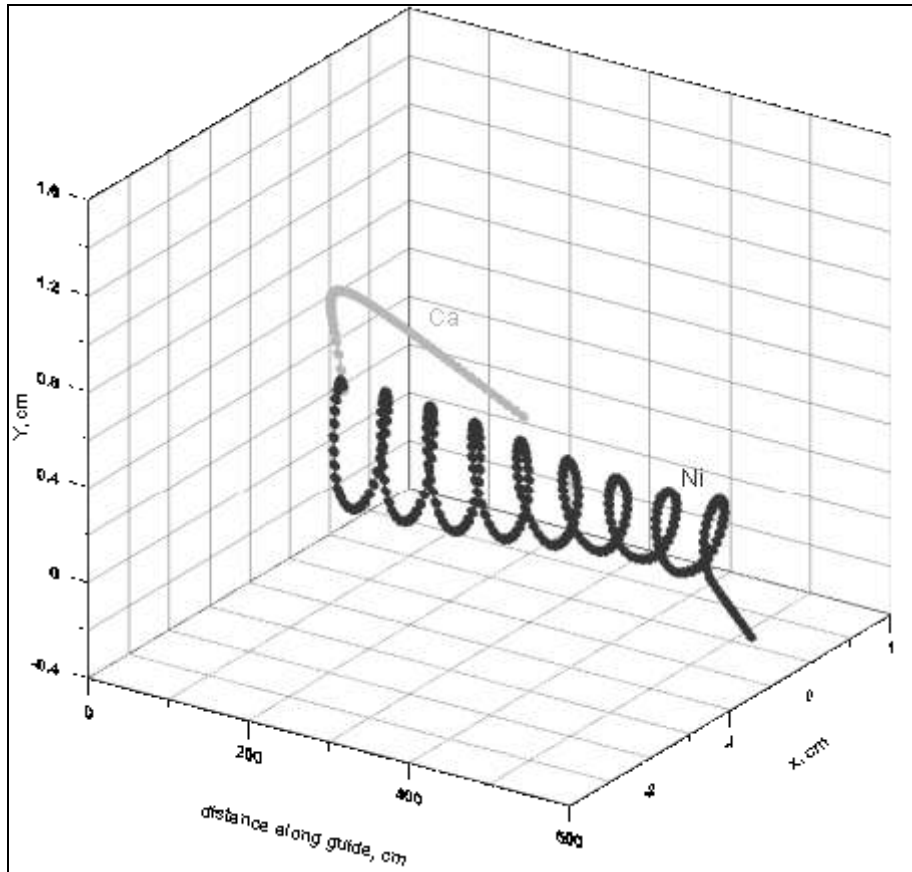


**FIGURE 5.** The 3D model trajectories of the initially collinear ions of Ca and Ni emitted at  $\beta_{max}(Ca)$ .

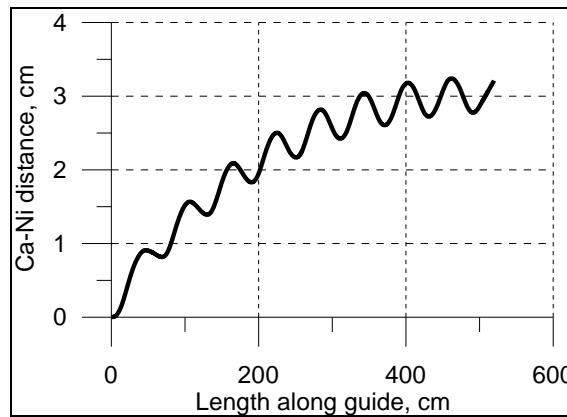


**FIGURE 6.** The distance between the ions of Ca and Ni in the plane perpendicular to the central electrode as a function of the length from the target. Ions of Ca and Ni started from the target at  $\beta_{max}$  corresponding to these ions.

The length of the flight-pass between the “start” detector and the “stop” mosaic of PIN diodes must be taken into account for correct estimation of the distances between Ca and Ni ions on the mosaic. We placed the registration system approximately 20 cm ( $L2 + L3=20$  cm) distant from the end of the guide (fig. 3b). The resulted spectrum of distances between initially collinear pairs of Ni and Ca at the detector position is shown in fig. 7.

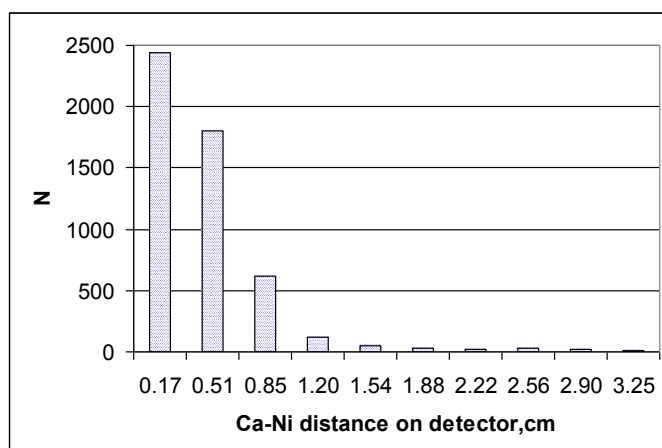


**FIGURE 7.** Spectrum of distances at the mosaic plane between initially collinear ions of Ca and Ni.

Total number of 6912 pairs of the ions emitted at the angles  $\beta_{max} \leq \beta_{max}(Ca)$  were analyzed. The number of detected Ca ions does not exceed 5286 since 66 and 1560 ions were missed on the tube wall and central electrode respectively. The number of detected Ni ions does not exceed 5216, the other 1696 ions were missed on the central electrode).

## PROSPECTS FOR REALIZATION

Some model layouts of the guide system at the IBR-2 reactor were considered (fig. 8).



**FIGURE 8.** The considered model layouts of the guide system at the IBR-2 reactor.

The first model layout comprises (“1” in fig. 8) the asymmetric fragment beam line of 8 meters in the left arm and 7 meters in the right one. The target chamber is three meters distant from the surface of the active zone.

The second layout (“2” in fig. 8) of the system consists of the central target chamber  $120 \times 120 \times 120 \text{ mm}^3$  and two beam lines of 7 and 5 meters long. The target chamber is located in the vicinity of the reactor channel 4 placed at 5.3 meters from the surface of the active zone. The beam line is parallel to the floor of the circular corridor.

The last, and the most realistic layout (fig.8, “3”) coincides with the location of the existing through channels 1 and 9.

Depending on the layout above the thermal neutron flux expected at the target position will amount to  $10^{10} \div 10^{12} \text{ cm}^{-2} \text{ s}^{-1}$ .

The preliminary design of the experimental chamber at the end of the guide system is shown in fig. 9.

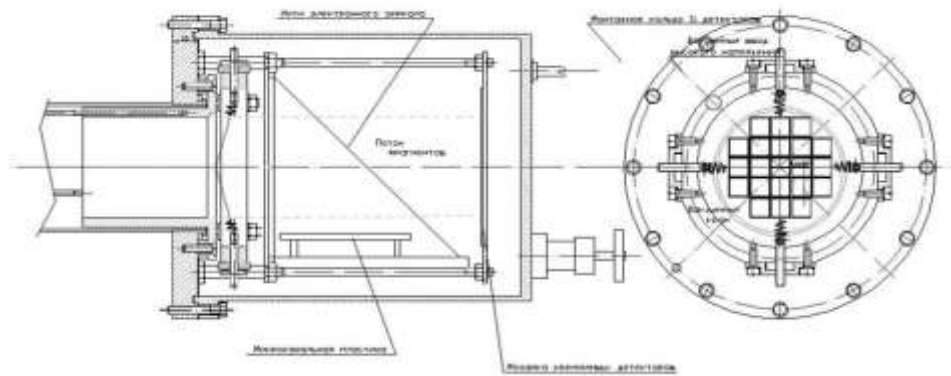


**FIGURE 9.**  
The design of the  
experimental  
chamber.

## CONCLUSIONS

Modeling of the transport of the initially collinear fragments along the electrostatic guide system lets come to following conclusions.

1. Due to the action of the guide the pairs of initially collinear ions can get space dispersion (fig. 7). This provides the possibility of their independent registration in the “stop” mosaic at the end of the guide.
2. The guide system should play a role of a “velocity-filter” providing an essential time delay between the signals from the ions from the same CCT pair in both the timing and energy detectors. This feature is useful for realization of the so called “double-hit” option for registration of two different fragments in the same detector.

## REFERENCES

1. D.V. Kamanin et al., Int. J. Mod. Phys. E. 2008. V. 17, No. 10. P. 2250–2254.
2. Yu.V. Pyatkov et al., Eur. Phys. J. A. 2010. V. 45. P. 29–37.
3. Yu.V. Pyatkov et al., Bulletin of the Russian Academy of Sciences. Physics. 2011. V. 75. P. 949–952.
4. A.A. Alexandrov et al., NIM A. 1991. V. 303. P. 323–331.
5. N.C. Oakey, P.D. McFarlane, NIM. 1967. V. 49. P. 220–228.